4A.6 *A METHOD FOR EXTRACTION OF CLOUD MICROPHYSICAL PROPERTIES USING A CONTINUOUS WAVELET TRANSFORM OF CLOUD RADAR SPECTRA: PRELIMINARY RESULTS*

Guo Yu*, Johannes Verlinde, Eugene E. Clothiaux, Giovanni Botta, Kultegin Aydin

Pennsylvania State University, University Park, PA

Alexander Avramov, Andrew S. Ackerman, and Ann M. Fridlind

NASA Goddard Institute for Space Studies, New York, New York

Introduction

Clouds have important impacts on atmosphere radiation and hydrological cycle. In mixed-phase clouds, liquid and ice can coexist. Mixed-phase clouds have a major presence in global cloud cover [*Hogan et al.*, 2004]. Some previous studies indicate mixed-phase clouds occur approximately 45% of the time in the Arctic [*Shupe et al.*, 2006], with maximum occurrence during the transition seasons. These Arctic mixed-phase clouds are typically stratiform, occur at the top of the inversion-capped boundary layer and can persist for days, even weeks. The radiative properties and life cycle of mixed-phase clouds are sensitive to the partitioning of cloud phase. The liquid in mixed-phase clouds usually plays a dominant role in cloud-surface radiative interactions [*Shupe and Intrieri*, 2004]. Mixed-phase clouds are understudied compared to single-phase clouds because of the observational limitations. In-situ measurements are hindered that aircrafts are not able to fly through mixed-phase clouds because of the icing hazard. Furthermore, the satellite retrievals of clouds at high latitudes are often hampered by the ice-covered ground.

* *Corresponding author and address*: Guo Yu, Penn State Univ., Dept. of Meteorology, State College, PA, 16803; email: gxy904@psu.edu.

The state of our ability to characterize the properties of mix-phase clouds are briefly discussed here. First, the most successful retrieval of mixed-phase clouds information is of the macrophysical properties. Combining the data from active and passive measurements, we can obtain robust and consistent results of cloud boundaries. Second, layer averaged properties of ice can be obtained by data analysis from different sources. Millimeter wavelength cloud radars (MMCR) are widely used because they can penetrate and detect multiple cloud layers. Radar return responds to particle size to the sixth power, making it particularly useful to the detection of large ice particles. There are different ice retrieval methods being used by previous studies [*Daniel et al.*, 2006; *Donovan et al.*, 2001; *Matrosov et al.*, 2002; *Shupe et al.*, 2006]. The magnitude of difference between retrieval methods suggests uncertainties on the order of a factor of 2, which is in agreement with other uncertainty estimates based on comparisons with aircraft in situ observations [*Matrosov et al.*, 2002; *Shupe et al.*, 2005].

Liquid detection in mixed-phase cloud is more challenging than ice retrieval because radar returns are usually dominated by the large ice particles, lidar signals cannot reach farther than the area near cloud base, and radiometer measurements can only provide the layer-averaged value. Currently, there is no widely

applicable liquid retrieval algorithm. The best generalized method for liquid detection is a scaled adiabatic LWC assumption, which can be computed using temperature soundings and cloud boundaries identified by radar and lidar [*Illingworth et al.*, 2007; *Zuidema et al.*, 2005]. The purpose of this paper is to propose a potential method to detect liquids in mixed-phase clouds based on radar measurements.

Data and method

In order to evaluate the newly developed liquid characterizing algorithm, we generate a number of radar Doppler spectra by a forward model of radar spectra simulator. We use simulated radar Doppler spectra data to testify and quantify the performance of our algorithm. To simulate radar Doppler spectra, firstly, we calculate the quiet radar spectra from the particle size distributions (PSD) for each class of hydrometeors (cloud drops, snow and aggregates) and their backscattering cross-sections [*Botta et al.,* 2011]. These PSDs are provided by a cloud resolving model (CRM) [*Avarmov et al.,* 2011]. Next, these quiet radar spectra are convolved by the mean vertical velocity and sub-grid vertical velocity variance in each model grid cell. Finally, we add noise to the convolved radar spectra by Zrnic's spectral simulator [*Zrnic*, 1975]. The statistical comparison of the radar moments (reflectivity, mean Doppler velocity, spectral width, skewness and kurtosis) between simulated radar Doppler spectra and observations indicates that the simulated radar spectra are realistic.

The rationale for detecting liquid is the assumption that radar Doppler spectra can be represented by a linear superposition of Gaussian distributions (termed 'modes' in the following), every mode being produced by a discrete class of hydrometeors with characteristic fall velocity [*Melchionna et al.*, 2008]. To localize the center for each mode is the key of separating spectral peaks. The continuous wavelet transform (CWT) analysis has the ability to find those centers. We apply a second-order Gaussian CWT to the simulated radar spectra. The result of applying CWT to a radar Doppler spectrum is a two dimensional array providing feature localization in both Doppler velocity and spectral width (scale).

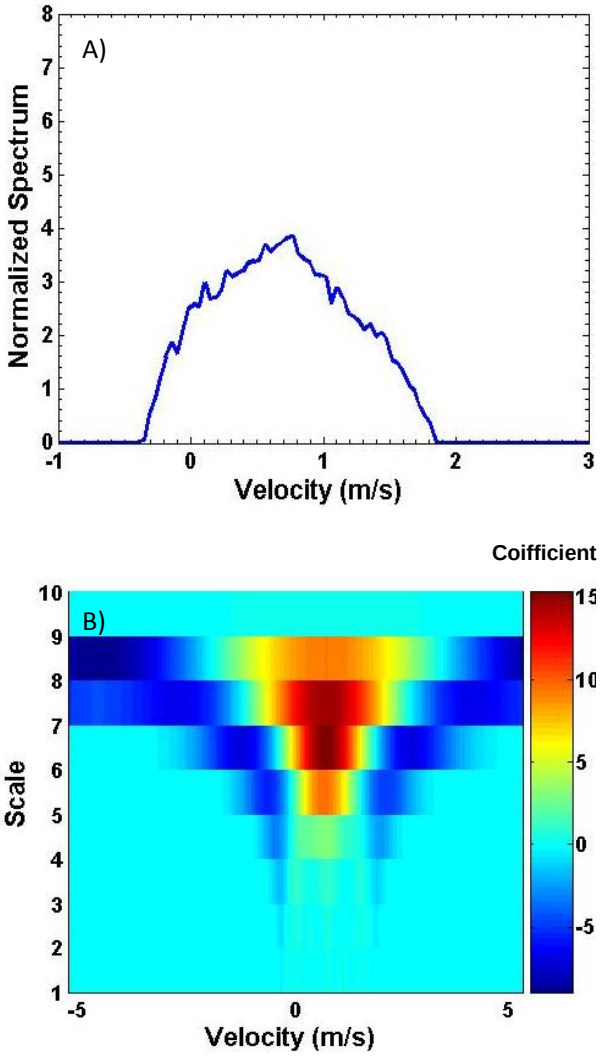

Figure 1. (A) Example of a simulated mixed-phase Doppler spectrum, (B) the corresponding wavelet transform of the Doppler spectrum at each scale

Results

Fig.1A presents a typical mixed-phase cloud spectrum with skewness less than zero (spectrum tilt towards the low fall velocity edge) due to the presence of both liquid and ice particles in the radar sample volume. The CWT analysis is applied to Fig.1A on 10 different scales and the resulting coefficient formed Fig.1B. The maximum value in the coefficient map indicates the main component to the sample Doppler spectrum locates at 0.5 m/s with a scale around 6. Except the obvious maximum value, there is a regional maximum value near fall velocity 0 m/s corresponding to the minor peak formed by liquid drops. We use the regional maximum values to locate the possible locations of liquid mode.

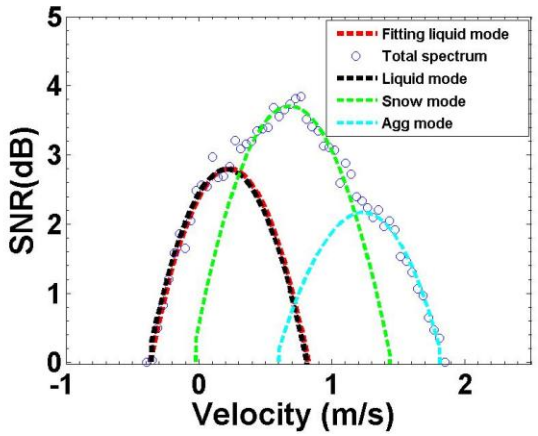

Figure 2. The fitting curve of liquid mode for a sample radar Doppler spectrum.

One of the fall velocity value from the left among those possible locations obtained by CWT analysis will be treated as the center of liquid mode. Combining with the data points of reflectivity on the radar Doppler spectrum, we fit the left edge of the radar spectrum based on a Gaussian model (Fig2). The fitting curve (red dashed line) fits the liquid mode (black dashed line) pretty well, and captures the important characteristics of the liquid mode, such as the center location and the peak value.

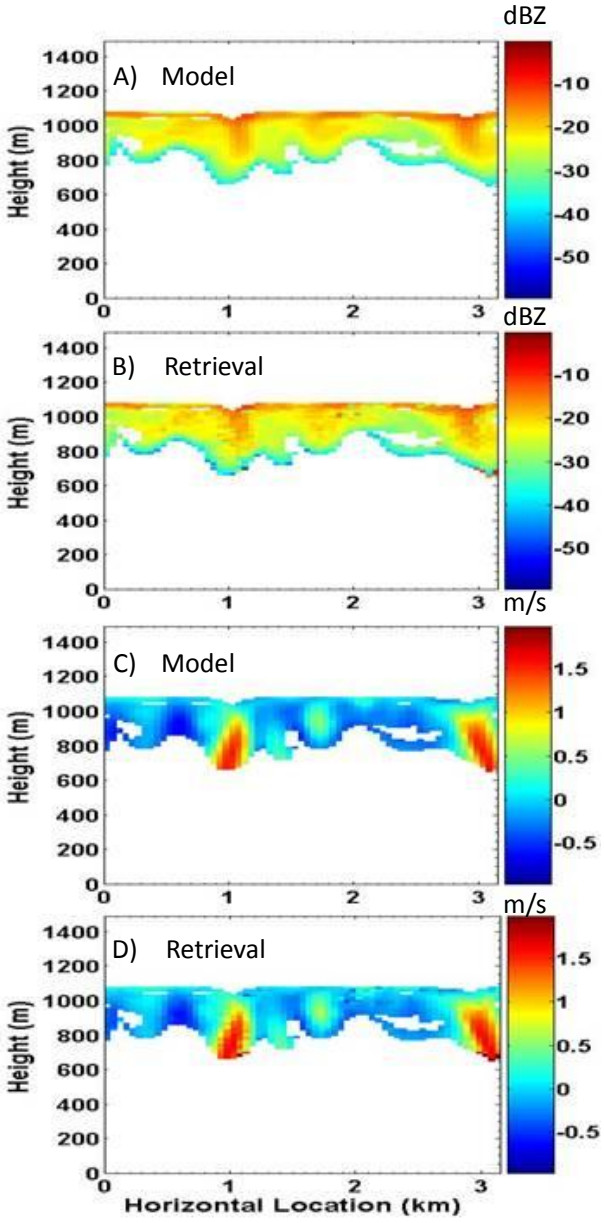

Figure 3. Comparisons between the retrievals and the true values on reflectivity due to liquids (A and B) and quiet air motion (C and D).

In order to evaluate the performance of our retrieval algorithm, we calculate the reflectivity from liquid and the vertical air motion based on the fitting curve of the liquid mode, and then compare

them with the input values from the CRM model. The reflectivity due to liquid are calculated by summing up all the area below the fitting liquid mode curve and the vertical air motion is estimated by the center of the fitting liquid mode. Fig3.A and B indicate most of the retrieved liquid reflectivities are consistent with the model inputs in a cross section of the cloud layer. The reflectivity from liquid is proportional to the liquid amount. Thus, liquid in the cloud layer increases with height and the majority of liquid locates near the cloud top. Our algorithm can characterize the vertical profile of liquid water properties. Fig3. C and D also demonstrate that our liquid retrieval algorithm can seize the updraft and downdraft regions in the cloud. Also the magnitudes of the vertical air motion are quiet close between model inputs and the retrieved value.

Fig4 presents the performance of our algorithm in a cross section of the cloud layer. The relative error histogram of the reflectivity from liquid shows the retrieval difference between retrieved liquid amounts and the input values from the CRM model has been constrained within a factor of 2, which is at a same uncertainties level of cloud ice retrieval. It can be also found that our algorithm tends to underestimate the liquid amount slightly. In the absolute error histogram of the retrieved vertical air motion, the retrieval is overestimation. Part of the reason is because our retrieval value includes the vertical air motion and the fall speeds of the small liquid droplets, while the original model value contains only the air motion. Although the fall speeds of small liquid droplets can be neglected in most circumstances, it can cause some bias in the retrieving process.

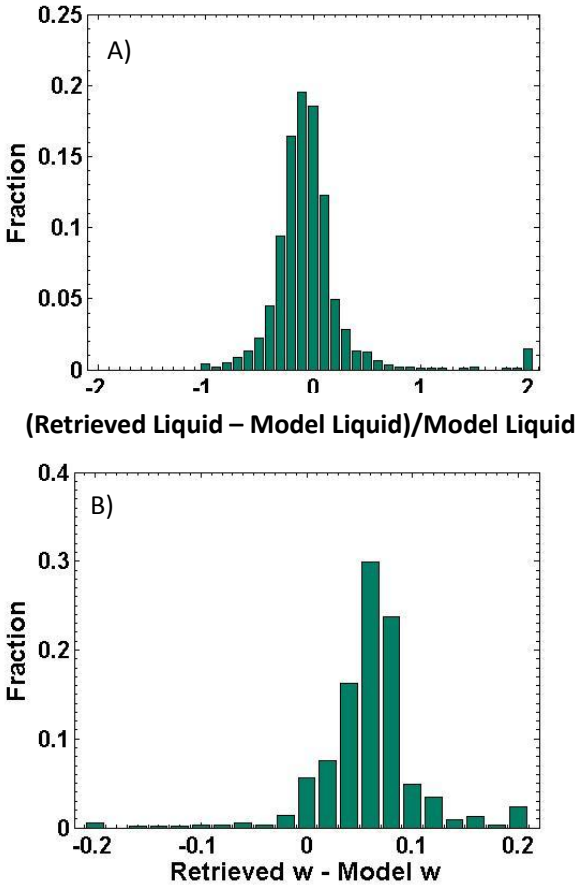

Figure 4. Histogram of the errors between retrieved values and model inputs on reflectivity due to liquid and vertical air motion.

Conclusion

The radiative properties and life cycle of mixed-phase clouds are sensitive to the phase of their hydrometeors. Cloud radars are widely used to detect the vertical profile of cloud structure. However, detection of liquid by radar is challenging because radar signal is dominated by large ice particles. Here we propose an algorithm that potentially can overcome this deficiency.

Using the results of a cloud resolved model, we simulate a number of radar Doppler spectra. The retrievals of reflectivity due to liquid and vertical air motion based on these simulated radar

Doppler spectra agree with the inputs from the CRM model. The difference between the retrieval liquid amounts and the inputs from the model is constrained to a factor of 2. But the algorithm tends to underestimate the liquid amount and overestimate the vertical airmotion.

In our future work, we will try to quantify the error sources. Thus we can make appropriate adjustments based on our current results. Eventually, this method will be applied on radar observation.

Reference

Botta, G. et al, Millimeter Wave Scattering from Ice Crystals and Their Aggregates: Comparing Cloud Model Simulations with X- and Ka-Band Radar Measurements, *J. Geophys. Res.,*doi:10.1029/2011JD015909, in press.

Daniel, J., et al. (2006), Cloud property estimates from zenith spectral measurements of scattered sunlight between 0.9 and 1.7 mm, *J. Geophys. Res*, *111*.

Donovan, D. P., et al. (2001), Cloud effective particle size and water content profile retrievals using combined lidar and radar observations - 2. Comparison with IR radiometer and in situ measurements of ice clouds, *Journal of Geophysical Research Atmospheres*, *106*(D21), 27449-27464.

Hogan, R., et al. (2004), Estimate of the global distribution of stratiform supercooled liquid water clouds using the LITE lidar, *Geophys. Res. Lett*, *31*.

Illingworth, A., et al. (2007), Continuous evaluation of cloud profiles in seven operational models using ground-based observations, *Bull. Am. Meteorol. Soc*,*88*, 883?898.

Matrosov, S. Y., et al. (2002), Profiling cloud ice mass and particle characteristic size from Doppler radar measurements, *Journal of Atmospheric and Oceanic Technology*, *19*(7), 1003-1018.

Melchionna, S., et al. (2008), A new algorithm for the extraction of cloud parameters using multipeak analysis of cloud radar data - First application and preliminary results, *Meteorologische Zeitschrift*, *17*(5), 613-620.

Shupe, M., and J. Intrieri (2004), Cloud radiative forcing of the Arctic surface: The influence of cloud properties, surface albedo, and solar zenith angle, *Journal of Climate*, *17*(3), 616-628.

Shupe, M., et al. (2006), Arctic mixed-phase cloud properties derived from surface-based sensors at SHEBA, *Journal of the Atmospheric Sciences*, *63*(2), 697-711.

Shupe, M. D., et al. (2005), Arctic cloud microphysics retrievals from surface-based remote sensors at SHEBA, *Journal of Applied Meteorology*, *44*(10), 1544-1562.

Zrnic, D. S. (1975), Simulation of weatherlike Doppler spectra and signals, *Journal of Applied Meteorology*, *14*, 619.

Zuidema, P., et al. (2005), An arctic springtime mixed-phase cloudy boundary layer observed during SHEBA, *Journal of the Atmospheric Sciences*, *62*(1), 160-176.